

Supramolecular Metalloglycodendrimers Selectively Modulate Lectin Binding and Delivery of Ru(II) Complex into Mammalian Cells.

Harikrishna Bavireddi,^[a] Raghavendra Vasudeva Murthy,^[a] Madhuri Gade,^[a] Sivakoti Sangabathuni,^[a] Raghavendra Kikkeri*^[a]

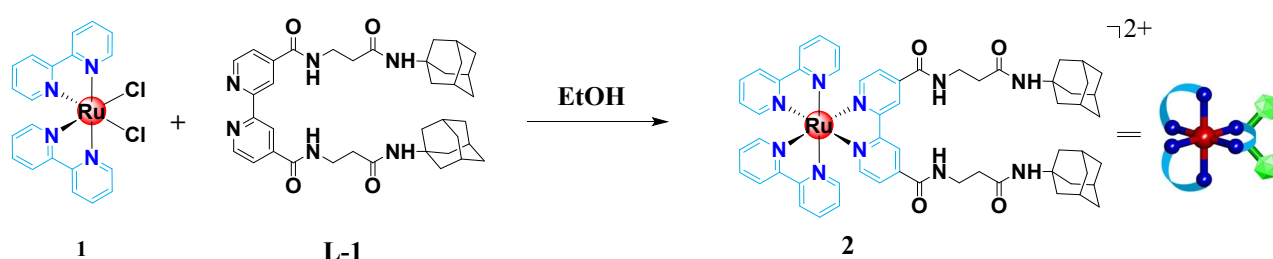
1. General Information
2. Synthesis of Ru(II) complex
3. Synthesis of complexes 3 to 5
4. Characterization of complexes 3 to 5
5. Isotherm titration calorimetry (ITC)
6. UV-Visible spectra
7. Fluorescence spectra
8. Stability of the host-guest complexes.
9. Confocal laser scanning microscopy images
10. NMR and 2D spectra

1. General Information

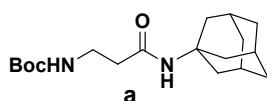
Commercial grade reagents and solvents were used without further purification except as indicated below. Deionized water was obtained from an in-house purification system. Analytical thin layer chromatography (TLC) was performed on Merck silica gel 60 F254 plates (0.25 mm) and visualized by UV or by dipping the plate in CAM solution followed by heating. Medium pressure column chromatography was carried out on Fluka Kieselgel 60 (230–400 mesh). ¹H and ¹³C NMR spectra were recorded on Jeol 400 MHz and 100 MHz respectively using the residual solvents' signals as internal references (for CDCl₃: δ_{H} , 7.26 ppm, δ_{C} 77.3 ppm and for CD₃OH: δ_{H} 3.31 ppm, δ_{C} 49.0 ppm). Chemical shifts (δ) are reported in *ppm* and coupling constants (*J*) in Hz. DMEM media and 3-(4, 5-dimethylthiazol-2-yl)-2, 5-diphenyltetrazolium

bromide (MTT) were purchased from Invitrogen and Sigma-Aldrich respectively. HeLa, HepG2 and NIH-3T3 cells were obtained from the National Centre for Cell Science (NCCS), Pune. High resolution mass spectra (HRMS) were recorded with an Agilent 6210 ESI-TOF mass spectrometer. UV/Vis spectra were recorded with an Ultrospec 6300 pro UV/Visible Spectrophotometer (GE Healthcare, Amersham Biosciences, Piscataway, NJ, USA). Fluorescence spectra were recorded with LS 55 fluorescence spectrometer (Perkin Elmer, MA, USA). All measurements were performed in ultra-pure water or in methanol HPLC grade (VWR, Darmstadt, Germany).

2. Synthesis of Ru(II) complex



Scheme S1: Synthesis of **2**

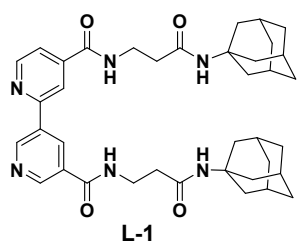


tert-butyl (3-((3*s*,5*s*,7*s*)-adamantan-1-ylamino)-3-oxopropyl)carbamate (a).

1-Adamantylamine (1.0 g, 6.62 mmol) and Boc-alanine (1.4 g, 7.2 mmol) were dissolved in DCM (60 mL) at r.t. DIC (1.0 g, 7.94 mmol) was then added, followed by the addition of DIPEA (2.1 g, 16.5 mmol). The reaction mixture was stirred at r.t for 12 h. The product was then extracted with EtOAc (70 mL) and the organic layer was washed with H₂O (2×50 mL). The resulting organic layer was then dried over MgSO₄, filtered, concentrated, and the crude

was purified by flash column chromatography (silica gel, DCM:MeOH 19:1) and dried under *high vacuo* to give the final product (1.5 g, 71%) as a white foam.

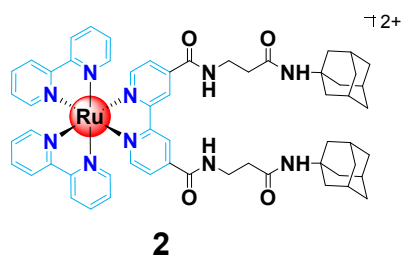
R_f 0.72 (DCM:MeOH 19:1). ¹H NMR (CDCl₃, 400 MHz) δ_H: 5.29 (s, 1H), 5.21(s, 1H), 3.37 (q, *J*= 8 Hz, 2H), 2.32 (t, *J*= 8 Hz, 2H), 2.07 (s, 3H), 1.98 (d, *J*= 4Hz, 6H), 1.67 (t, *J*= 4Hz, 6H), 1.43 (s, 9H). ¹³C NMR (CDCl₃, 100 MHz) δ_C: 170.42, 155.96, 79.00, 51.89, 41.46, 36.88, 36.62, 36.13, 29.21, 28.24; HRMS (ESI, positive mode) calc'd. for C₁₈H₃₀N₂O₃[M+H]⁺: 323.2334; found: 323.2339.



***N*⁴,*N*⁵-bis(3-((3*s*,5*s*,7*s*)-adamantan-1-ylamino)-3-oxopropyl)-[2,3'-bipyridine]-4,5'-dicarboxamide (L-1).**

Under an Ar atmosphere, 2,2'-bipyridine-4,4'-dicarboxylic acid (100 mg, 1.23 mmol) and SOCl₂ (5.0 mL, 42.6 mmol) were mixed together at r.t. to give a white suspension. The reaction mixture was then heated under reflux over 2 d at 60 °C to give a clear green solution. Excess of SOCl₂ was removed by vacuum distillation at 70 °C and the crude was dried under *high vacuo* to give 2,2'-bipyridine-4,4'-dicarbonyl dichloride as a green solid which was then dissolved in dry DCM (5 mL) under N₂ atmosphere, followed by the addition of adamantyl derivative **a** (340 mg, 4.6 mmol). The resulting mixture was then treated dropwise with Et₃N to reach pH 8. The solution was stirred over 1 d at r.t. The solvent was then removed under reduced pressure and the residue was then purified by flash column chromatography (silica gel, DCM:MeOH 19:1 to 9:1), and dried under *high vacuo* to give **L-1** (100 mg, 37%) as a white solid.

R_f 0.45 (DCM:MeOH (9 : 1)). ^1H NMR (CDCl_3 , 400 MHz) δ_{H} : 8.98 (d, J = 8Hz, 2H), 8.91 (s, 2H), 7.94 (d, J = 4Hz, 2H), 3.83 (t, J = 8Hz, 4H), 2.65 (t, J = 8Hz, 4H), 2.22 (s, 6H), 2.17 (s, 12H), 1.85 (s, 12H). ^{13}C NMR (CDCl_3 , 100 MHz) δ_{C} : 172.41, 164.87, 156.74, 150.30, 141.66, 121.74, 118.71, 52.37, 41.71, 36.51, 36.28, 29.41. HRMS (ESI, positive mode) calc'd. for $\text{C}_{38}\text{H}_{48}\text{N}_6\text{O}_4\text{H}$ $[\text{M}+\text{H}]^+$: 653.3815; found: 653.3812.



cis-Bis(bipyridine){1,1'-(2,2'-bipyridine-4,4'-diyl)bis-3-β-ethane-(adamantane)ruthenium(II) (2).

Ligand **L-1** (52.0 mg, 79.7 μmol) was dissolved in EtOH (10 ml) at room temperature followed by *cis*-bis(2,2'-bipyridine)dichlororuthenium(II) hydrate (45.5 mg, 87.7 μmol) was added. The reaction mixture was then heated to 80 °C for 12h. The solvent was then removed under reduced pressure and the residue was then dissolved in CH_3CN . The crude product was then purified by flash column chromatography (silica gel, $\text{CH}_3\text{CN}/\text{sat. solution of KNO}_3$ 8 : 2 to 7 : 3), and dried under *high vacuo* and dissolved in a minimum of CH_3CN and filtered to remove salts. The precipitation was repeated three times to ensure complete removal of salt and the filtrate was then dried under *high vacuo* to give the product **2** (21.4 mg, 19.6%) as a red solid; R_f 0.35 ($\text{CH}_3\text{CN}/\text{sat. solution of KNO}_3$ 9 : 1). ^1H NMR (CDCl_3 , 400 MHz) δ_{H} : 9.13 (s, 2H), 8.74 (d, J = 8Hz, 4H), 8.18 (dd, J = 8Hz, J = 8Hz, 4H), 8.02 (t, J = 4Hz, 2H), 7.85 (m, 6H), 7.54 (m, 4H), 3.70 (t, J = 8Hz, 4H), 2.53 (t, J = 8Hz, 4H), 2.02 (bs, 18H), 1.70 (bs, 12H).

^{13}C NMR (CDCl_3 , 100 MHz) δ_{C} : 172.7, 165.5, 159.0, 157.6, 156.9, 152.0, 138.7, 127.7, 125.2, 124.3, 122.1, 51.4, 49.5, 40.8, 38.3, 37.5, 36.0, 30.9, 29.4. HRMS (ESI, positive mode) calc'd. for $\text{C}_{58}\text{H}_{64}\text{N}_{10}\text{O}_4\text{Ru} [\text{M}]^{2+}$: 1066.4156; found: 533.2077 $[\text{M}/2]^{2+}$.

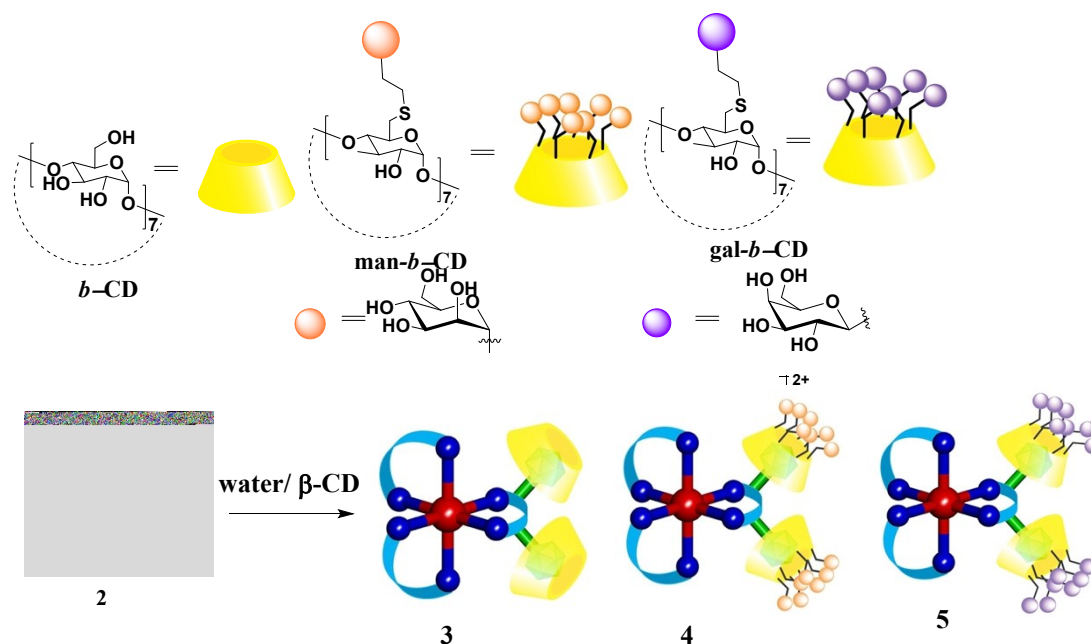
β -CD- mannose and β -CD-Glactose have been synthesized according to the literature procedure.¹

β -CD-Mannose and β -CD-Galactose NMR's:

β -CD-Mannose: 5.15 (bs, 7H), 4.92 (bs, 7H), 3.99-3.83 (m, 49H), 3.77-3.70 (m, 28H), 3.58-3.50 (m, 7H), 3.38-3.34 (m, 7H), 3.00 (bs, 21H).

β -CD-Galactose: 5.14 (bs, 7H), 4.92(bs, 7H), 3.99-3.79(m, 49H), 3.77-3.69 (m, 28H), 3.56-3.49 (m, 7H), 3.38-3.34 (m, 7H), 2.99 (bs, 21H).

3. Synthesis of complexes 3 -5.



Scheme S2: Synthesis of **3** to **5**

Synthesis of **3**:

Cis-bis(bipyridine){1,1'-(2,2'-bipyridine-4,4'-diyl)bis-3-β-ethane-(adamantane)ruthenium(II)} **2** (1 eq) was dissolved in MeOH (3 mL). β-Cyclodextrin or β-cyclodextrin-based *O*-α-mannoside or β-cyclodextrin-based *O*-β-galactoside (**2** eq) was added and the reaction mixture was kept at 22 °C for 12 h. The solvent was removed under reduced pressure and dried under high *vacuo*. The residue was dissolved in H₂O (3 mL) and lyophilized to afford **3** to **5** respectively as brown solids.

¹H NMR (D₂O, 400 MHz) δ_H: 8.77 (bs, 2H), 8.41 (m, 4H), 7.93 (m, 4H), 7.87 (m, 2H), 7.67 (m, 6H), 7.25 (m, 4H), 3.78 (m, 83H), 3.50 (29H), 2.44 (t, *J*= 8Hz 4H), 2.05 (bs, 12H), 1.92 (bs, 18H).

Theoretical Elemental Analysis: C (51.12), H (6.16), N (4.20), O (35.49), Ru (3.03).

Observed Elemental Analysis: C (49.98), H (5.91), N (4.01), O (34.07).

Similarly we have synthesised **4** and **5** also.

Theoretical Elemental Analysis for **4**: C (47.32), H (6.25), N (2.17), O (35.73), Ru (1.57) S (6.96).

Elemental Analysis for **4**: C (45.92), N (2.09), O (34.75).

Theoretical Elemental Analysis for **5**: C (47.32), H (6.25), N (2.17), O (35.73), Ru (1.57) S (6.96).

Elemental Analysis for **5**: C (46.07), N (2.13), O (34.62) S (6.77).

4. Characterization of complexes **3** to **5**

¹H-NOESY spectra:

NOESY spectrum of **3** displayed clear and strong nuclear Overhauser effect (NOE) from **H3** and **H5** of β -CD and the adamantyl skeleton indicating the encapsulation of adamantyl from **2** in the β -CD inner core as was reported by Grunstein et al.²

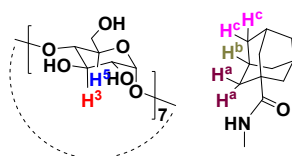


Figure S1. Proton designation of the relevant molecule moiety involved in host-guest complex.

5. Isothermal calorimetric titration.

In order to gain an insight into the binding affinity and thermodynamics and stoichiometry of the **4** and **5**. We performed isothermal calorimetry (ITC). The Man- β -CD and Gal- β -CD were titrated into the **2** in the calorimeter cells. Upon forming complex between β -CD and **2** heat is released, yielding a typical titration isotherm. Based on the qualitative assessment, **2** binding isotherm was fitted to a binding model containing one set of binding sites. The values of formation constants (K) and thermodynamic parameters determined by ITC are summarized in Table 1, where ‘N’ represents the number of **2** on the β -CD that are available for binding.

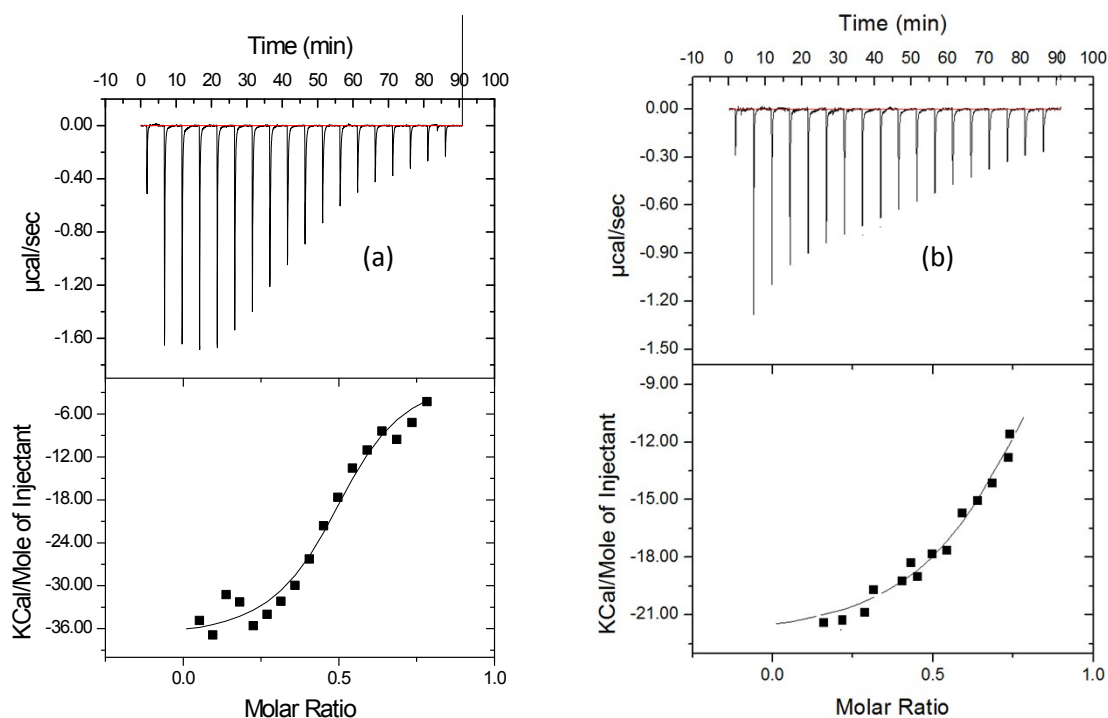


Figure S2. ITC profile for the interaction of Man- β -CD/2 (a) and Gal- β -CD/2 (b).

Host-guest complexes	n	Binding constant (M^{-1})	ΔH (Kcal/mol)	ΔS (cal/mol/deg)
2 vs Man- β -CD	0.47	3.64×10^2	-1.04 ± 0.12	-3.12×10^3
2 vs Gal- β -CD	0.46	2.12×10^2	-2.01 ± 0.42	-4.33×10^3

Table S1. Binding parameters.

6. Uv-visible spectra:

UV-visible spectra of the complexes **2** to **4** in water displayed identical spectra at MLCT region and slightly different spectral profile at LC region. MLCT and LC band of the complexes were observed at 475 nm and 350 nm respectively (Fig. S2).

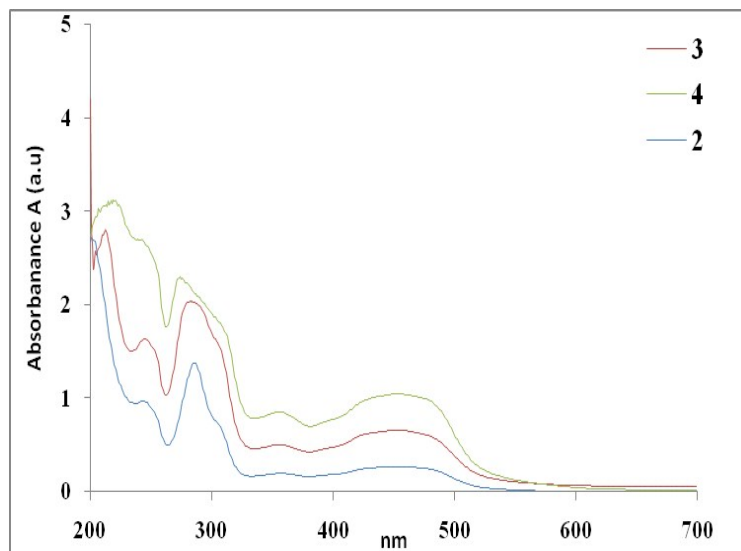


Figure S3. Absorption spectra of Ru(II) complexes in water

7. Fluorescence Spectra:

The emission spectra of the Ru series and the Ru-CD series exhibited an emission band at $\lambda_{\text{max}}^{\text{em}} \approx 650$ nm when excited at 450 nm. An increase in emission intensity and calculated quantum yield (Φ) directly correlates with the increasing complexity of the structures as more units of **2** and CD are assembled around the Ru(II) core

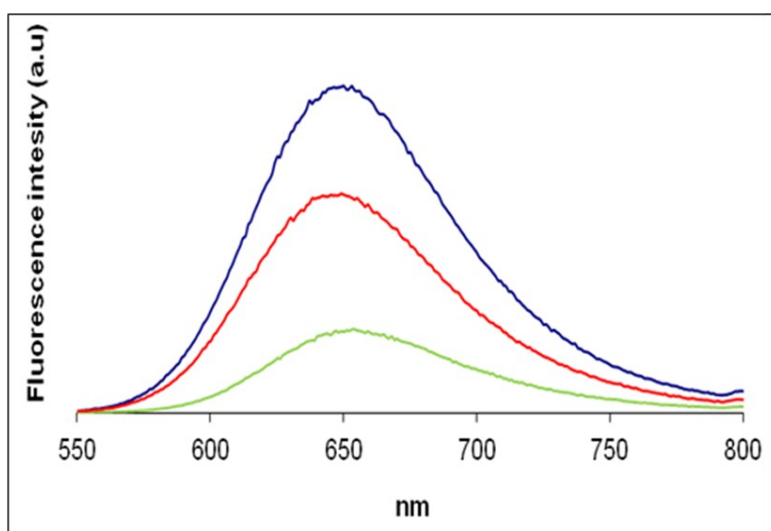


Figure S4. Fluorescent spectra of 2-4 complexes; **2** (blue line), **3** (red line) and **4** (green line).

	MLCT (nm)	ϵ (L. mol ⁻¹ . Cm ⁻¹)	$\lambda^{\text{em}}_{\text{max}}$ [nm]	QY (Φ) ²
2 in H ₂ O	462	4730	648	0.09
3 in H ₂ O	471	5073	652	0.22
4 in H ₂ O	470	5345	655	0.28

Table S2: Photophysical data of Ruthenium complexes

8. Stability of the host-guest complexes.

Since the stability in biological media due to interactions with proteins is a key factor in developing a new drug, we explored the stability of the newly prepared complexes **3** and **4** in DMEM sera. It was done by recording the UV-visible and fluorescence spectra followed by exploring the AFM images and comparing the collected data to that from aqueous solutions. Based on our results, (Fig. S3 & S4) compounds **3** and **4** are stable in serum with no significant decomposition for at least 72 hours. Furthermore, quantum yields and absorption coefficients at ~660 nm and 470 nm clearly revealed no significant differences for 3 days (Table S2), AFM images and topology studies in water and DMEM after 0.5 and 72 hours were identical (Fig 2). Similar experiments in NaOAc buffer (pH 0.5), a model for the cytoplasmic environment in cancer cells, clearly showed the absence of topology by the complexes and a significant decrease in quantum yields (Table S3), indicating that once **3** and **4** update into the cells, the host-guest complexes were segregated.

Compound	Time (hours)	solvent	λ_{\max}	Φ	
2		H ₂ O	648	0.14	
3			652	0.22	
4			655	0.28	
2		DMEM	650	0.13	
3			649	0.21	
4			649	0.26	
3	1		652	0.22	
4	1		654	0.25	
3	2		652	0.21	
4	2		654	0.26	
3	3		652	0.21	
4	3		654	0.25	
3	24		652	0.22	
4	24		654	0.25	
3	48		652	0.21	
4	48		654	0.24	
3	72		652	0.22	
4	72		654	0.25	
3			NaOAc	652	0.13
4			(pH 0.5)	654	0.12

Table S3. Photophysical data of the ruthenium complexes

9. Confocal laser scanning microscopy images

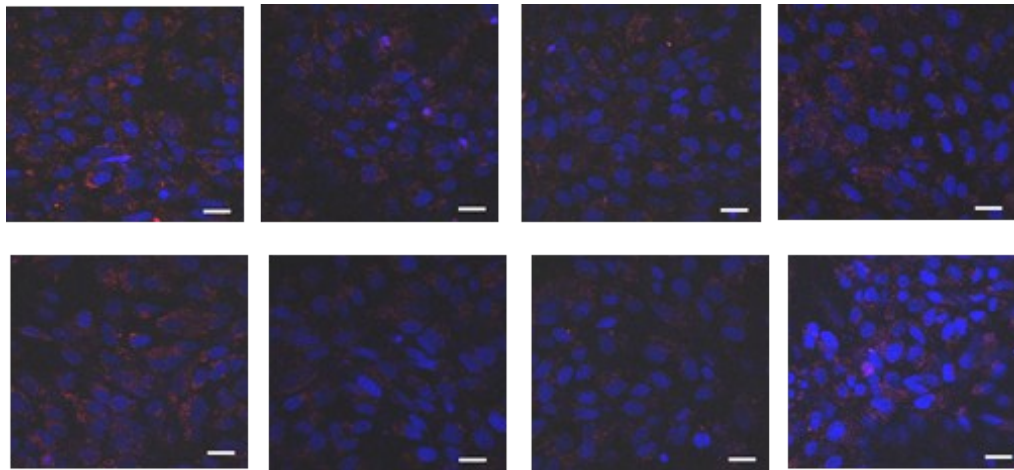


Figure S5. Fluorescence confocal microscopy images of NIH-3T3 cells treated with 50 μ M of **2** (a, e); **3** (b, f); **4** (c, g) and **5** (d, h) after 24 (a, b, c, d) and 48 (e, f, g, h), image scale 10 μ m. Staining with Hoechst 33342. Confocal fluorescence images were taken under identical conditions, magnification is 63 \times . scale bar = 10 μ m.

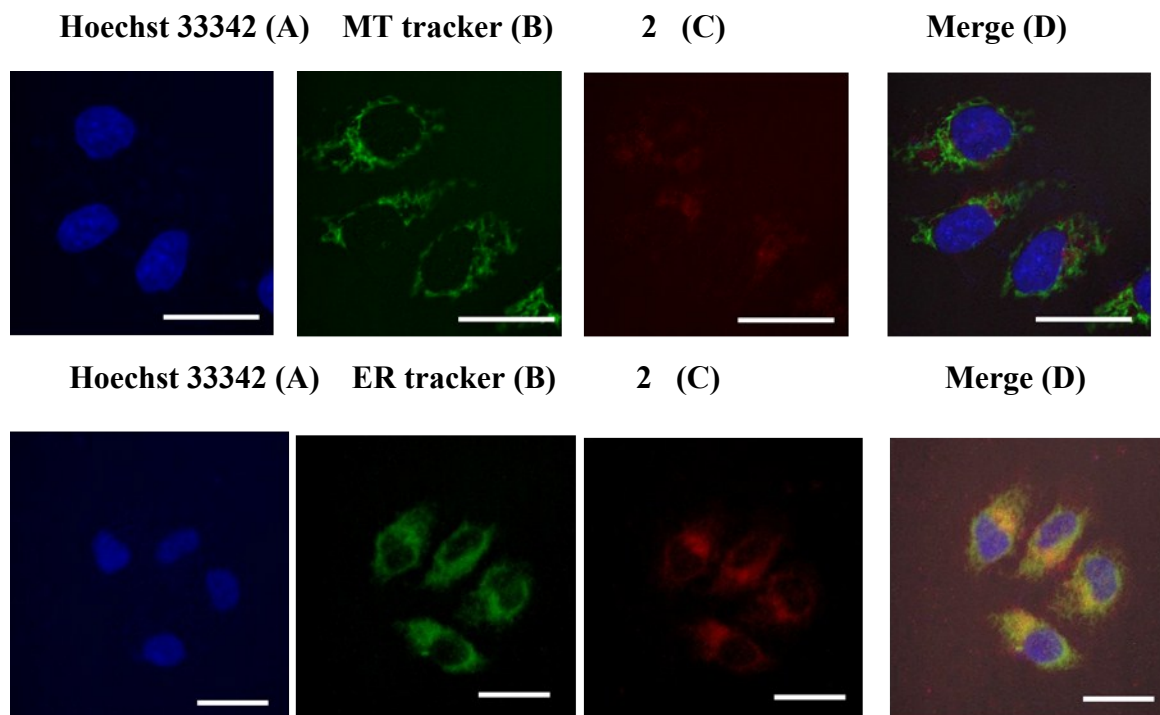
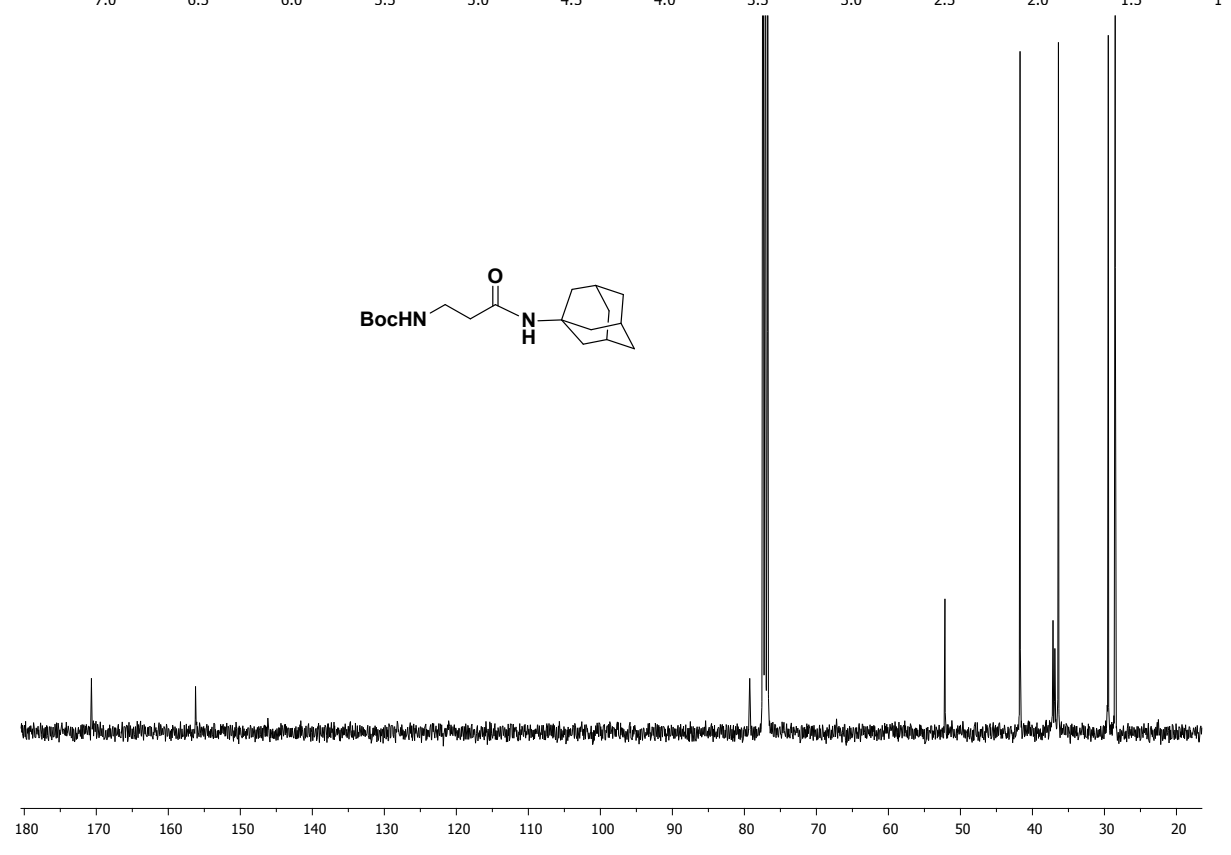
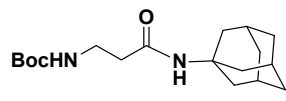
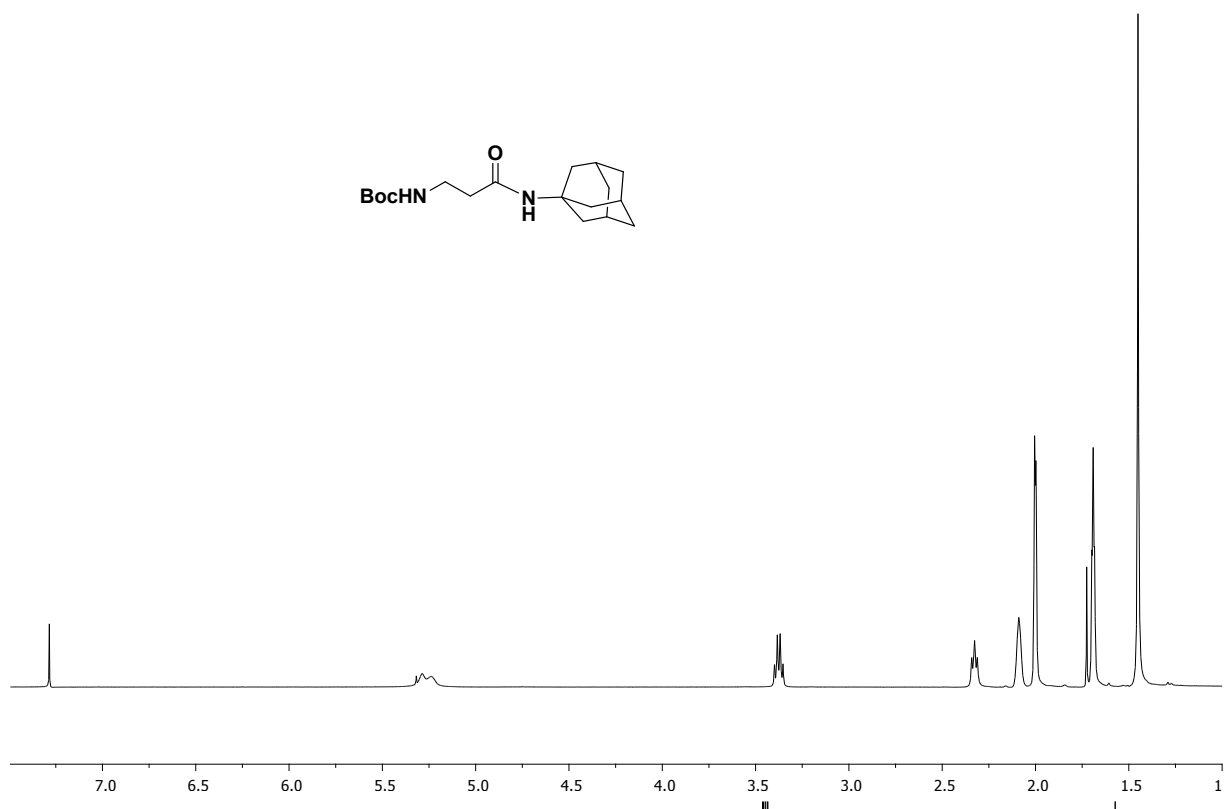
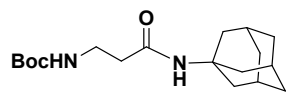


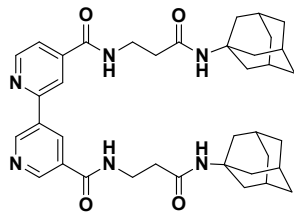
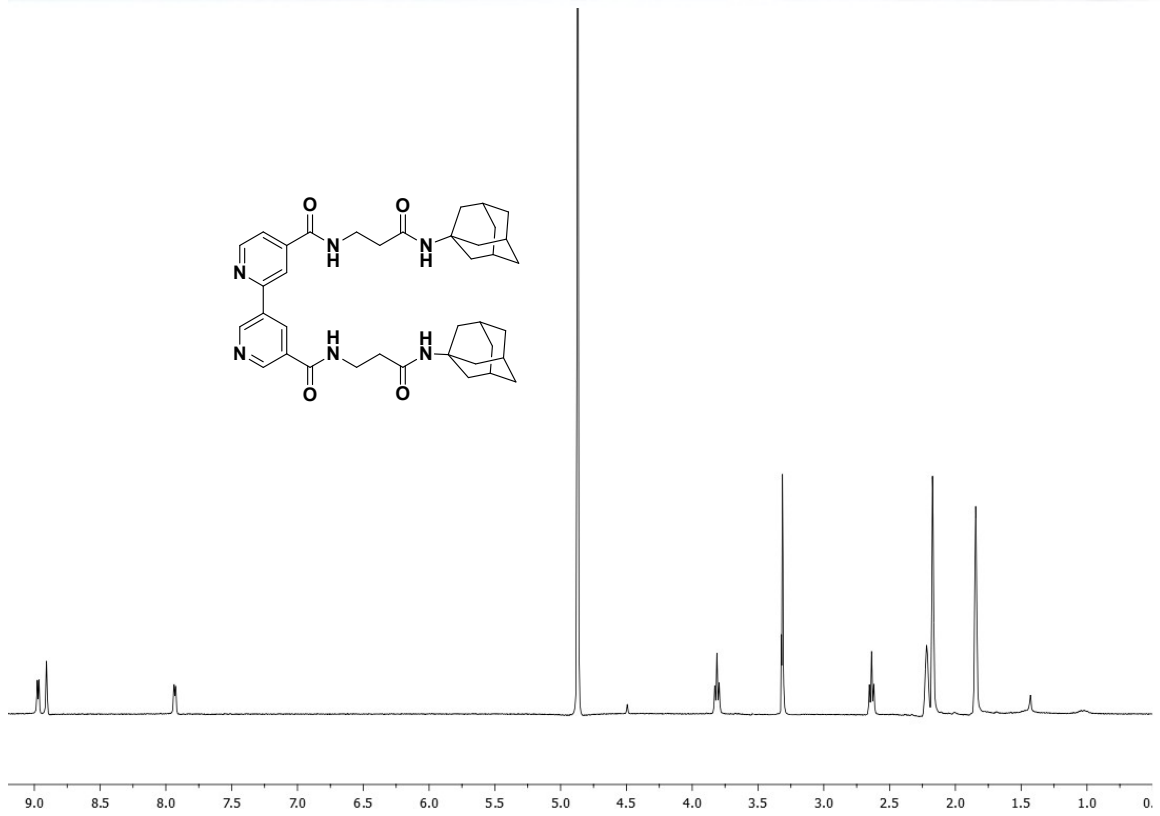
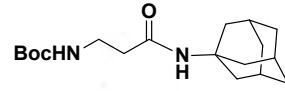
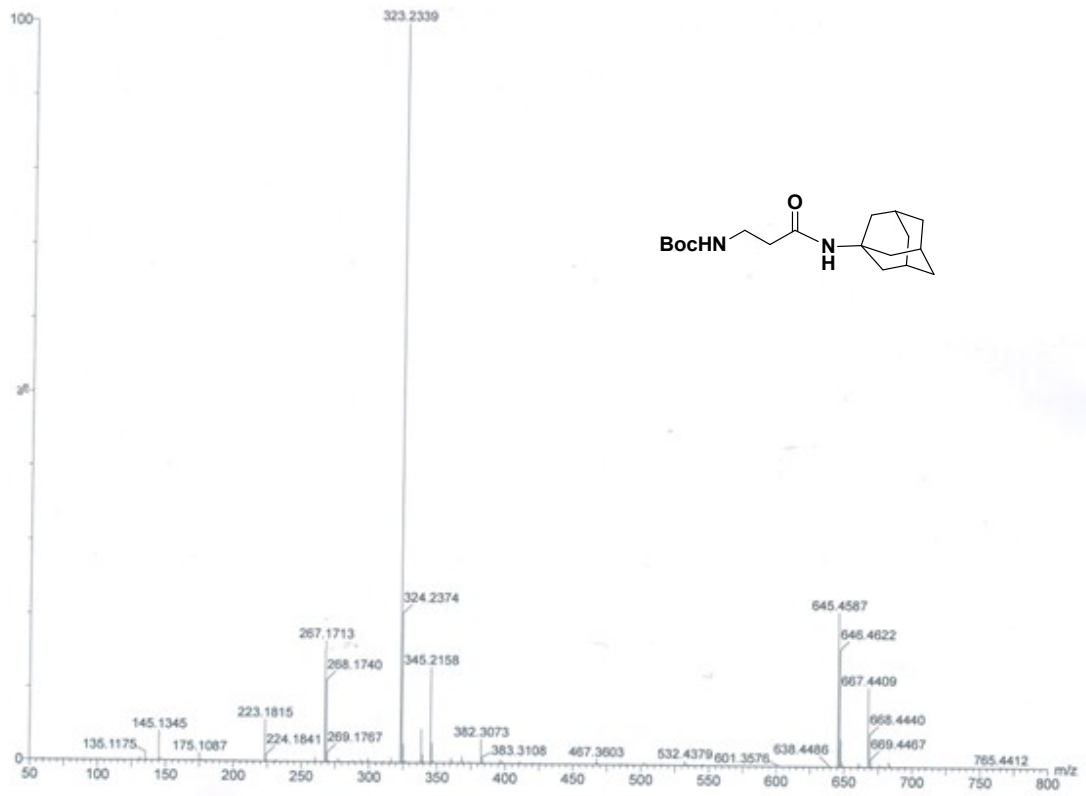
Figure S6. Confocal images of D- HeLa cells treated with **2** after 24 hours. Cells were incubated with 50 μ M of **2** for 24 h (red), rinsed, treated with ER Tracker or MT-tracker

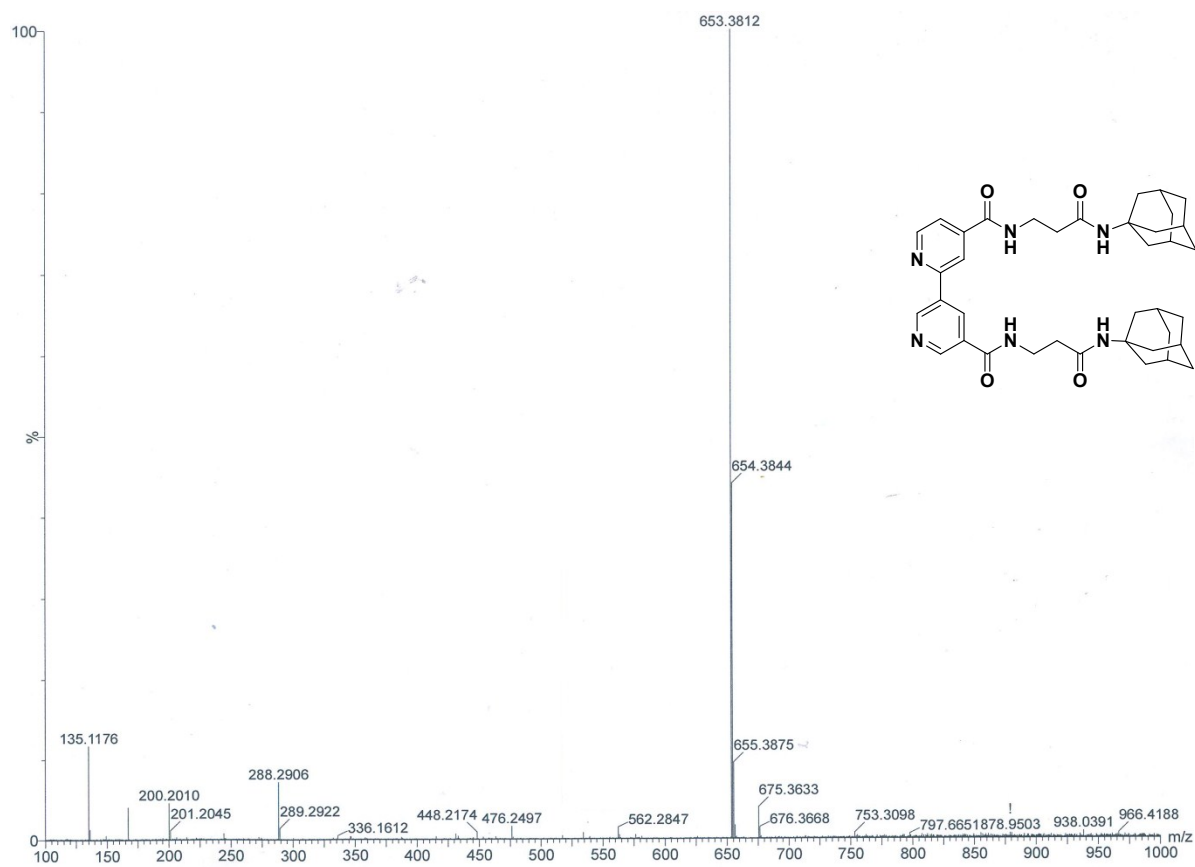
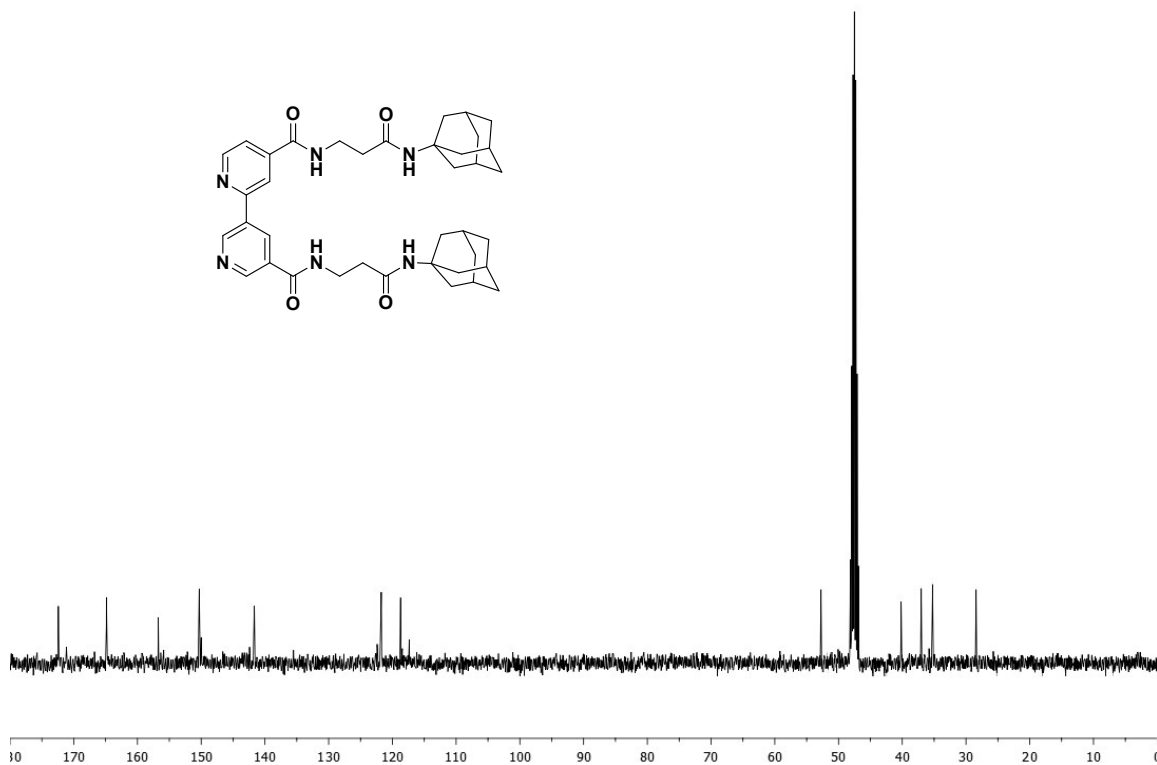
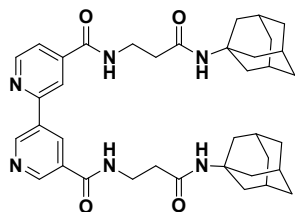
Green, rinsed Fluorescence of A: Hoechst 33342; Fluorescence of B: ER-Tracker or MT-Tracker Green; Fluorescence of C: **2** and Fluorescence of D: the overlapped image of A, B and C. Confocal fluorescence images were taken under identical conditions, magnification is 63 \times . scale bar = 10 μ m.

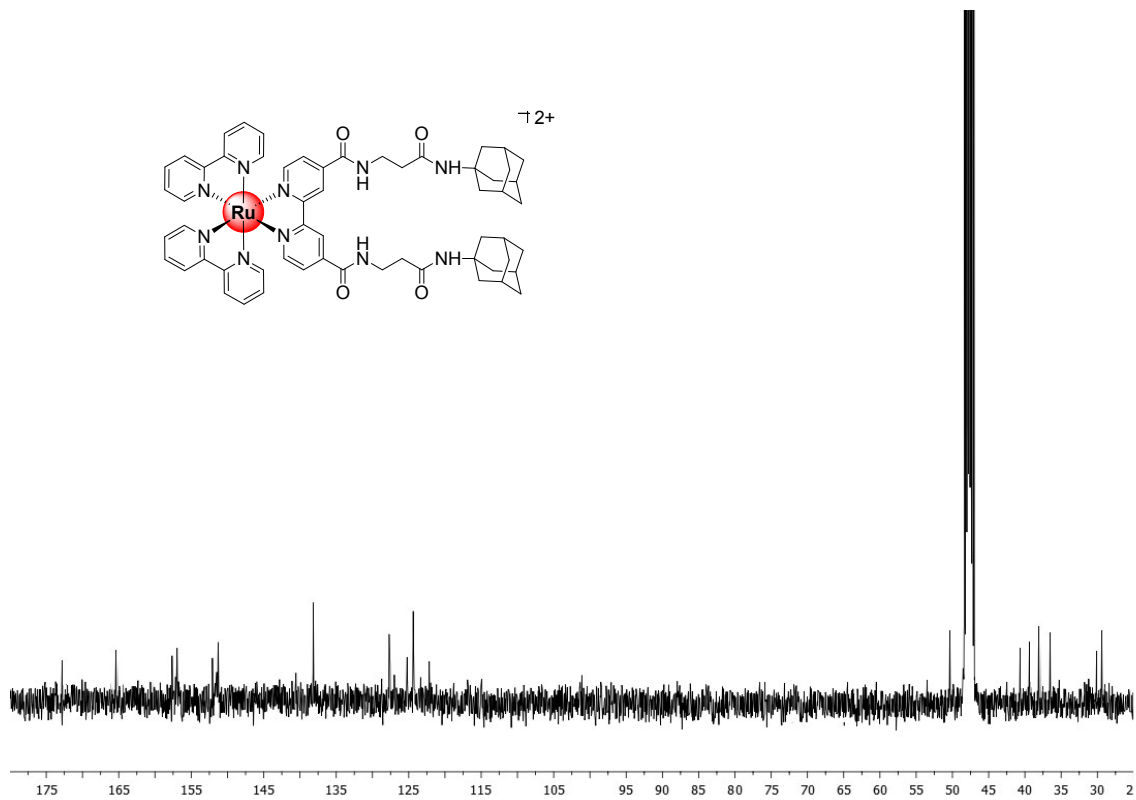
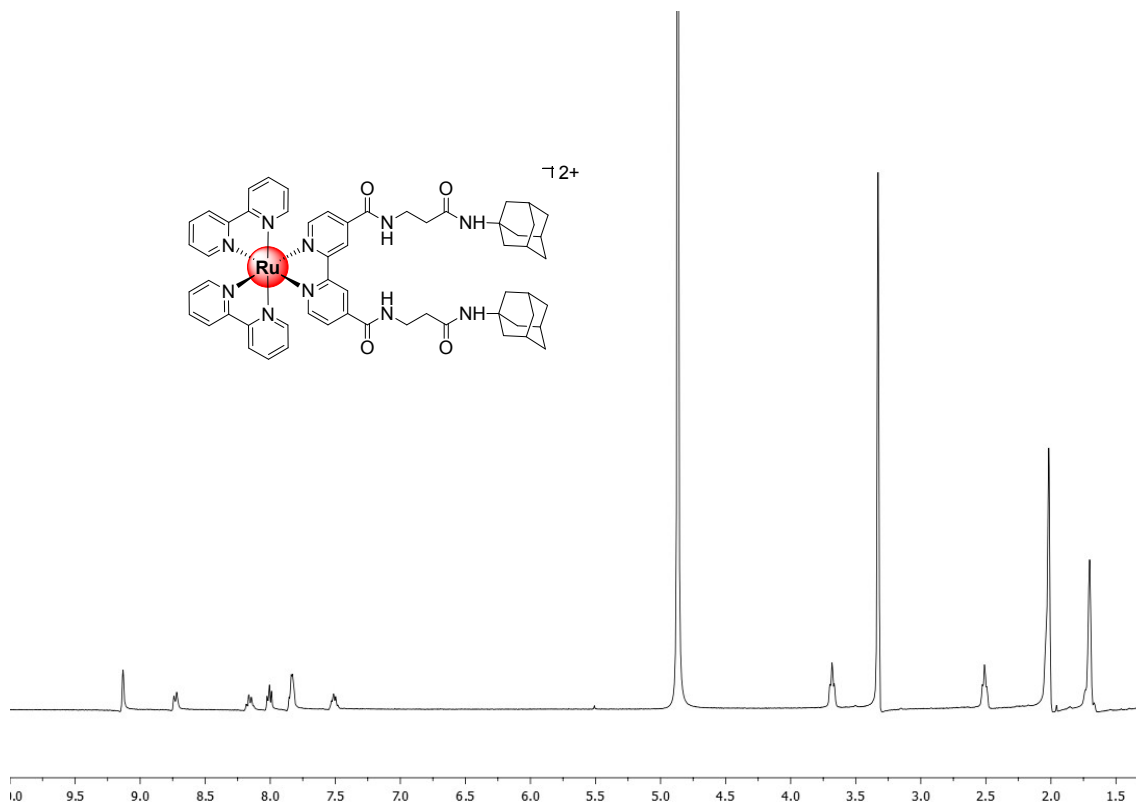
References

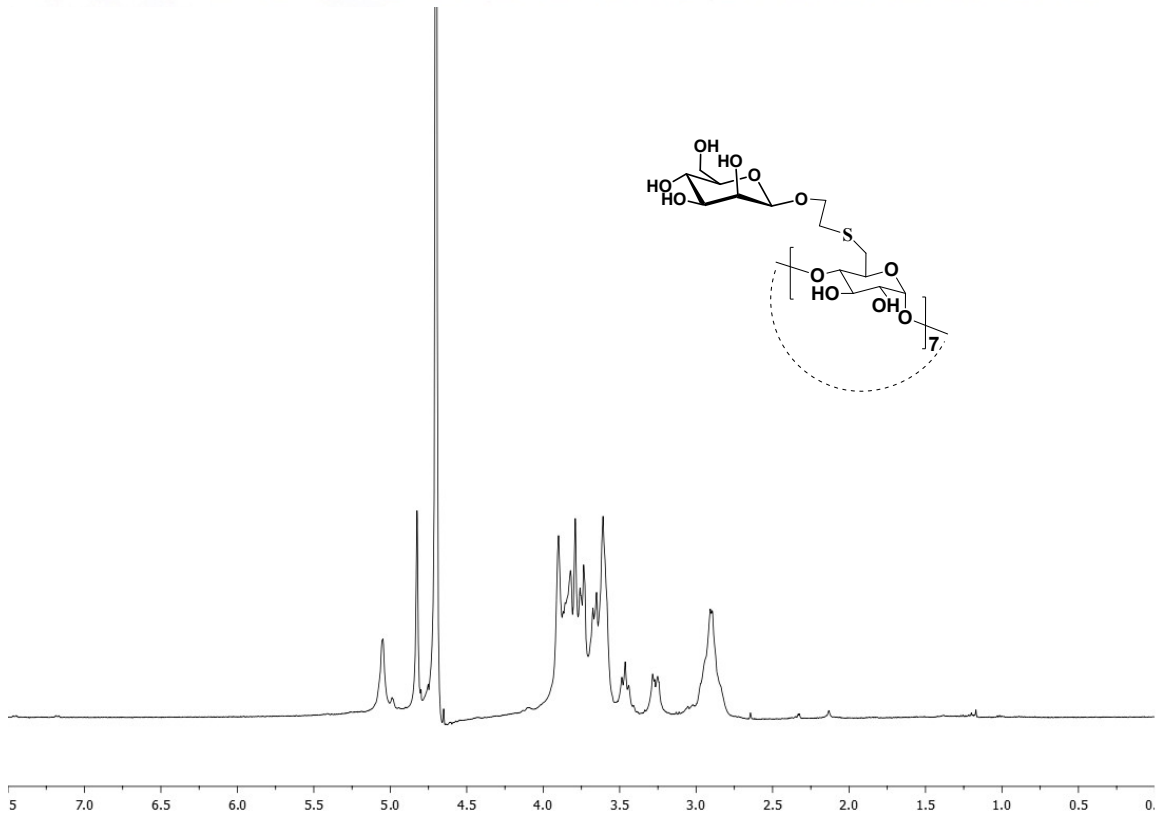
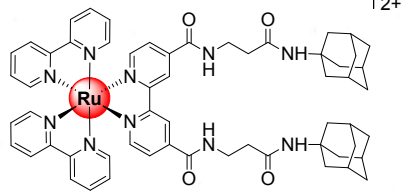
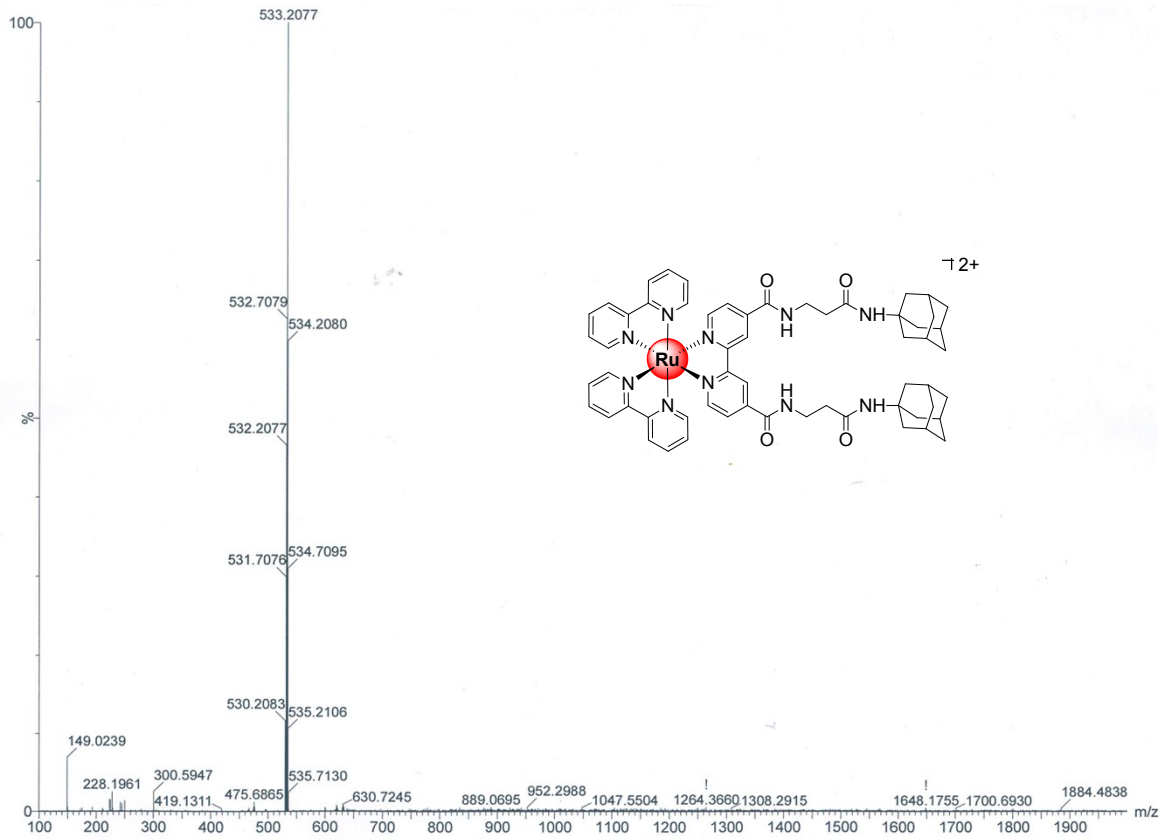
1. Bavireddi H, Kikkeri R (2012) *Analyst*, 137 5123-5127
2. Grunstein D, Maglinao M, Kikkeri R, Collot M, Barylyuk K, Lepenies B, Kamena F, Zenobi R, Seeberger P H (2011) *J Am Chem Soc* 133: 13957-13966

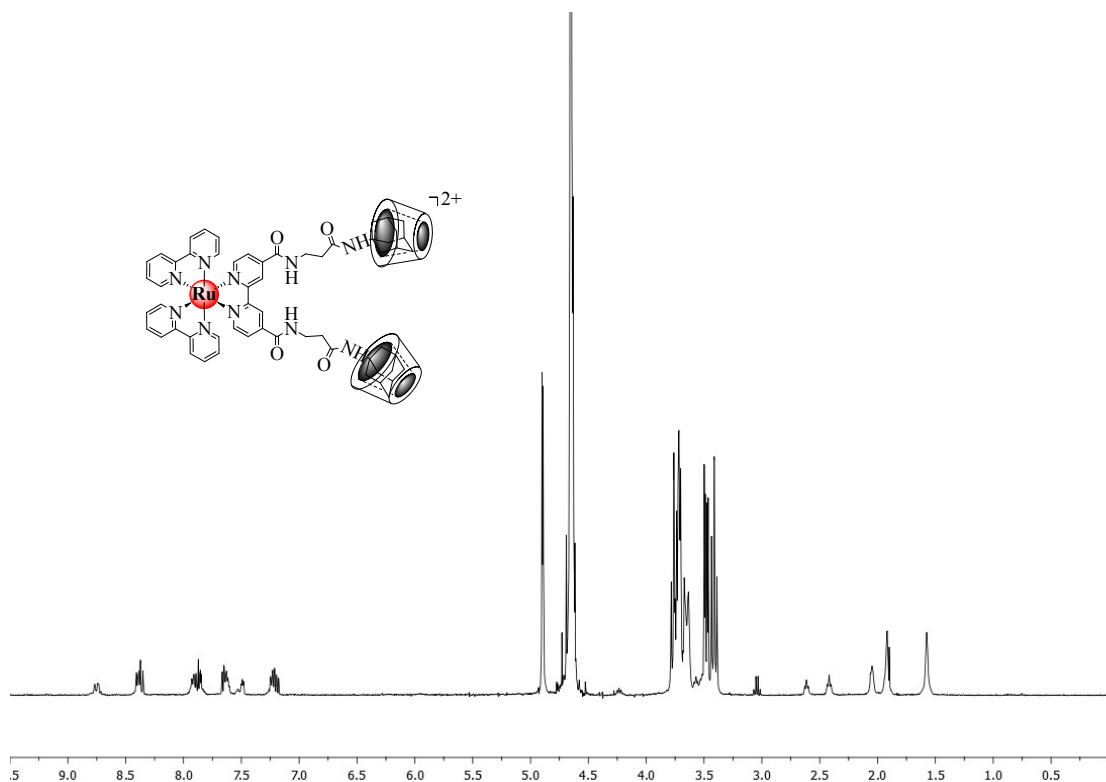
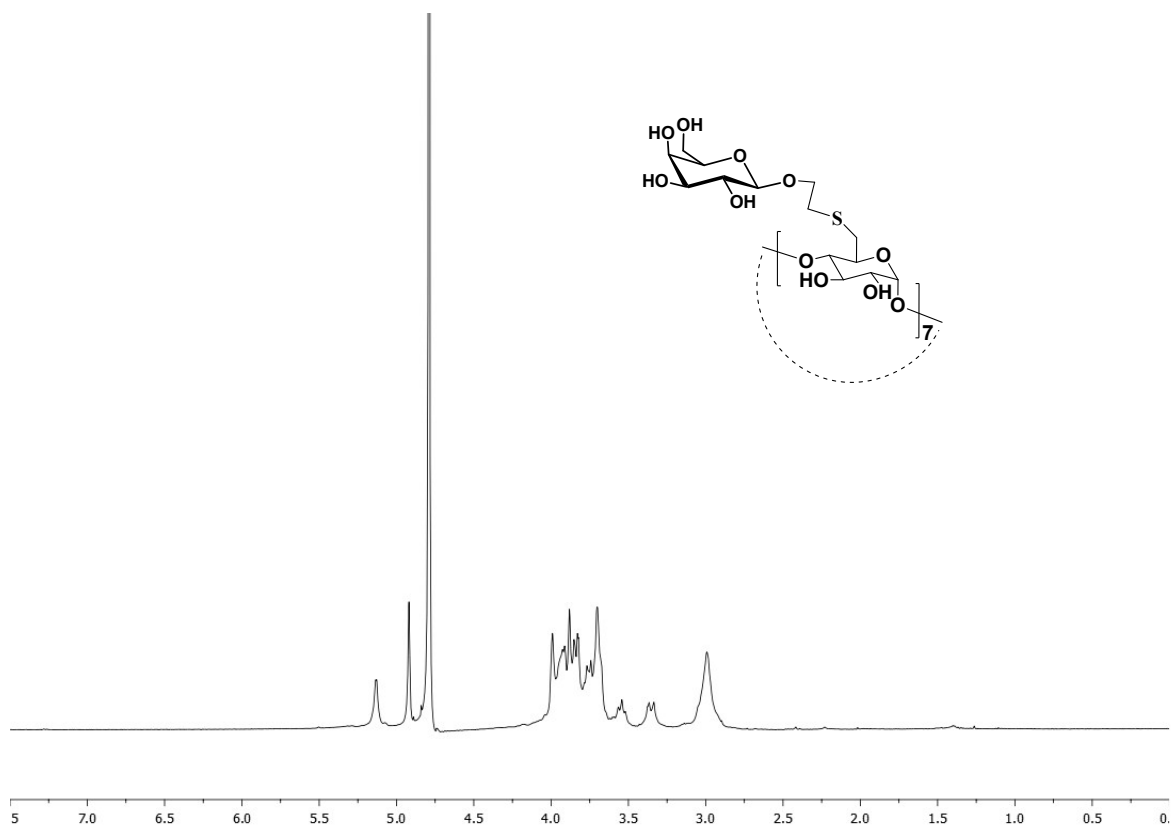


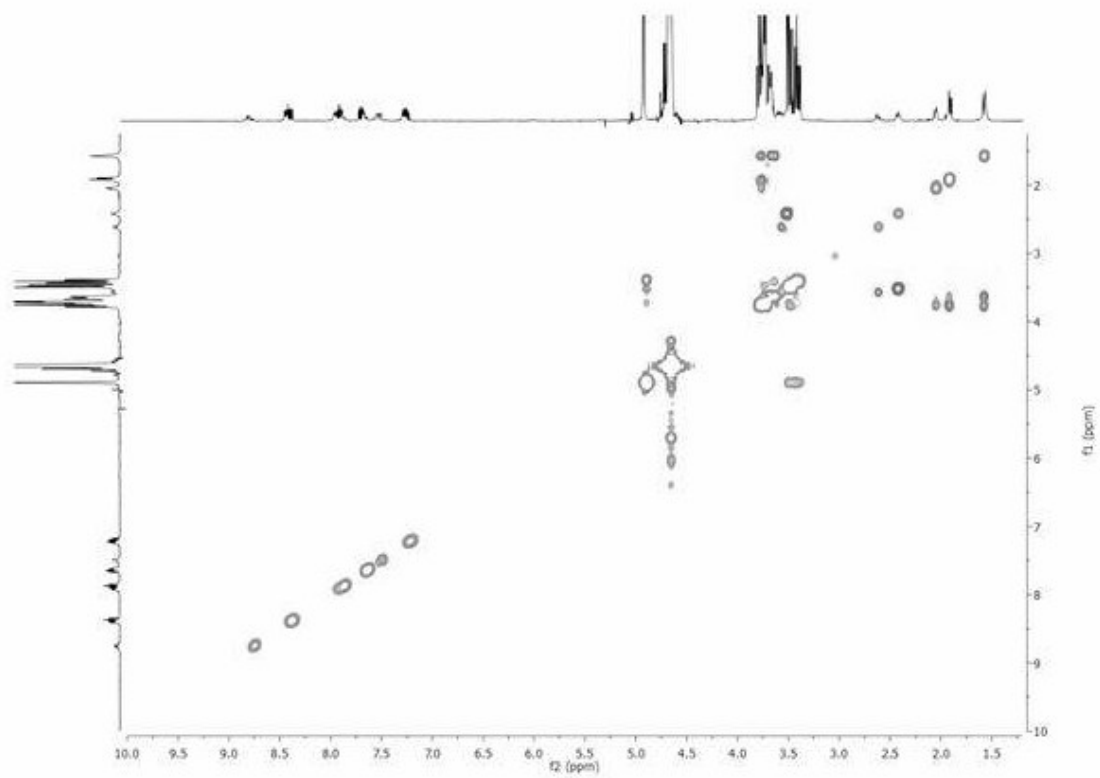




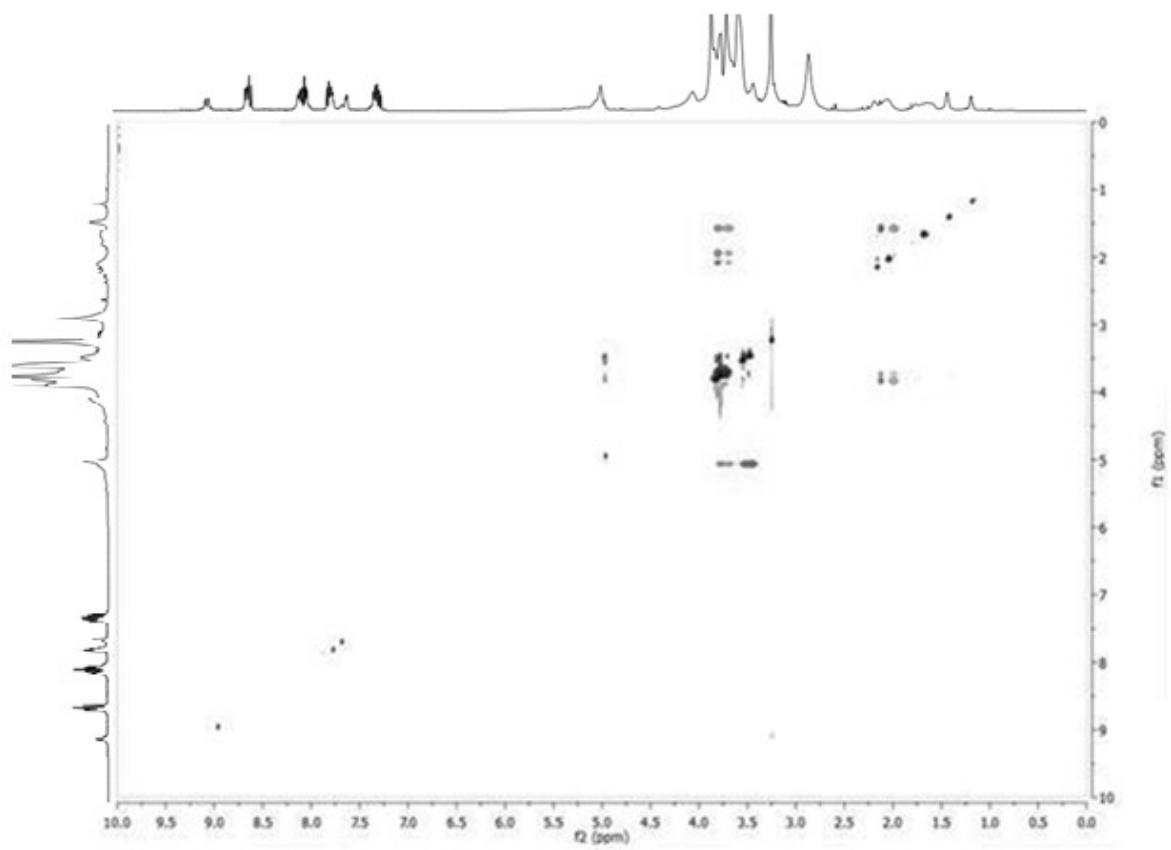








^1H -NOESY of **3**



^1H -NOESY of **5**